
One-Shot Hyper-Gradient Warm-Starts for Bandit-Style Hyperparameter Optimisation

Anonymous Author(s)

Affiliation

Address

email

Abstract

Bandit-style multi-fidelity schedulers such as ASHA and PASHA are the work-horses of practical hyperparameter optimisation, yet they still waste substantial compute on configurations that could have been flagged as poor before real training even begins. The root cause is that every trial is treated as a black box: none of the gradients already computed inside the training loop are exploited by the scheduler. We close this gap with One-Shot Hyper-Gradient Warm-Starts (OHGW). For each freshly sampled configuration we run exactly one mini-batch, obtain stochastic hyper-gradients $\frac{\partial L}{\partial \psi}$ for all continuous hyperparameters at almost zero extra cost via automatic differentiation, apply a single tiny update $\psi \leftarrow \psi - \eta_h \frac{\partial L}{\partial \psi}$, and hand the nudged configuration back to the unmodified scheduler. OHGW therefore preserves exploration while biasing every candidate toward lower-loss regions at negligible overhead and with no change to promotion or stopping logic. On CIFAR-10 with ResNet-20 under ASHA and on WikiText-103 with GPT2-small under PASHA, OHGW cuts median wall-clock time to a preset quality threshold by roughly twenty percent, adds under four percent floating-point operations, and leaves final accuracy and perplexity unchanged. Random perturbations provide almost no benefit and taking more than one hyper-step shows diminishing returns. These findings demonstrate that a single noisy hyper-gradient obtained before expensive training commences can reclaim a significant share of wasted computation in grey-box hyperparameter optimisation.

1 Introduction

Hyperparameter optimisation (HPO) is indispensable for obtaining robust performance in modern machine-learning systems, yet even the most popular grey-box schedulers squander a sizable fraction of their budget on clearly sub-optimal configurations. Successive-Halving variants such as Hyperband, ASHA and PASHA prune weak contenders early by evaluating them on progressively larger budgets Bohdal et al. [2022]. Grey-box Bayesian schemes like DyHPO refine this idea through learning-curve modelling and dynamic promotion rules Wistuba et al. [2022]. Despite these advances, almost all schedulers regard the training process itself as opaque: internal gradients that are already computed for parameter updates are ignored during the search.

Hyper-gradient methods have shown that gradients with respect to hyperparameters can be extracted cheaply via automatic differentiation Chandra et al. [2019] or implicit differentiation techniques that avoid expensive unrolling Bertrand et al. [2020]. Unfortunately these approaches typically assume full control over the optimisation routine and therefore clash with production HPO systems whose scheduling logic is complex and battle-tested. The open question, then, is how to inject very cheap but noisy hyper-gradient information into existing bandit-style frameworks without having to rewrite their core.

We address this question with One-Shot Hyper-Gradient Warm-Starts (OHGW). Whenever the scheduler samples a configuration $x = (\theta_0, \psi)$ consisting of model parameters θ (usually random initialisation) and continuous hyperparameters ψ , the training script performs exactly one forward-and-backward pass on a single mini-batch, collects the stochastic hyper-gradient $g_\psi = \frac{\partial L}{\partial \psi}$, and applies a microscopic update $\psi \leftarrow \psi - \eta_h g_\psi$ with $\eta_h = 10^{-3}$. Promotion rules, budgets and stopping criteria remain untouched; from the scheduler’s perspective nothing has changed except that the candidate starts from a slightly more promising point.

Two practical challenges arise. First, a gradient measured on a single mini-batch is extremely noisy, so the step must be sufficiently small to prevent biasing the search or harming exploration. Second, adoption hinges on a minimal engineering footprint ideally a few lines of code that do not depend on the internals of the scheduler. OHGW meets both constraints: the extra cost is one forward and one backward pass per trial ($< 4\%$ FLOPs in our experiments) and integration is a five-line wrapper around trial creation.

We validate OHGW in two contrasting settings vision (CIFAR-10, ResNet-20, ASHA) and language modelling (WikiText-103, GPT2-small, PASHA) using 56 paired random seeds and equal GPU budgets. Metrics include time-to-target quality, best final score, compute overhead, variance, and hyperparameter distribution shift. OHGW consistently shortens time-to-target by about twenty percent while preserving ultimate performance and introducing negligible bias. Ablations confirm that gradient directionality, not random perturbation, drives the gain, and that repeating the warm-start step gives only marginal additional savings.

1.1 Contributions

- **Scheduler-agnostic warm-start:** We introduce OHGW, a single-step hyper-gradient warm-start that improves efficiency without altering bandit logic.
- **Practical hyper-gradient extraction:** We provide a recipe for extracting hyper-gradients of continuous hyperparameters at negligible cost.
- **Consistent efficiency gains:** Experiments across vision and language reduce median wall-clock time to target quality by roughly twenty percent with under four percent compute overhead.
- **Robustness and ablations:** Gradient direction matters, benefits saturate quickly, and variance or bias are not inflated.

Looking forward, we plan to extend OHGW to mixed discrete/continuous spaces, integrate warm-start signals into surrogate-based selection Khazi et al. [2023] and adaptive-fidelity frameworks Jiang and Mian [2024], and explore privacy-aware or federated scenarios where one-shot, low-overhead interventions are especially attractive Panda et al. [2022], Khodak et al. [2021].

2 Related Work

2.1 Multi-fidelity schedulers

Successive-Halving, Hyperband and ASHA progressively allocate resources; PASHA adds an adaptive cap on maximum fidelity Bohdal et al. [2022]. DyHPO supervises the race among configurations with a deep-kernel Gaussian Process that embeds learning-curve dynamics Wistuba et al. [2022]. All these methods leverage intermediate metrics yet still initialise every configuration blindly. OHGW is complementary: it keeps the scheduling logic intact and instead improves the starting point of each trial.

2.2 Grey-box Bayesian optimisation

BOIL explicitly models iterative progress to balance cost and benefit Nguyen et al. [2019]. Deep Power Laws exploits power-law learning curves to decide when to pause training Kadra et al. [2023]. Deep Ranking Ensembles meta-learn surrogates that optimise ranking metrics Khazi et al. [2023]. Differentiable EHVI accelerates multi-objective acquisition optimisation with exact gradients Daulton et al. [2020]. These approaches rely on surrogate modelling and acquisition optimisation, whereas OHGW exploits native gradients already available in the training loop.

86 2.3 Gradient-based HPO

87 Early work showed how to compute hyper-gradients by augmenting backpropagation Chandra et al.
88 [2019]; implicit differentiation scales to non-smooth penalties Bertrand et al. [2020]; stochastic
89 marginal-likelihood gradients further reduce cost Immer et al. [2023]. These techniques operate
90 throughout training or require unrolling, imposing memory and engineering overhead. OHGW
91 applies a single pre-training step, trading precision for immediacy.

92 2.4 Data and fidelity efficiency

93 AUTOMATA speeds up HPO by selecting informative data subsets Killamsetty et al. [2022]; FastBO
94 adaptively chooses fidelities per configuration Jiang and Mian [2024]; DNN-MFBO and BMBO-
95 DARN model cross-fidelity correlations Li et al. [2020, 2021]. OHGW is orthogonal and can be
96 layered on top of any of these strategies.

97 2.5 Constrained settings

98 Federated HPO faces communication bottlenecks Khodak et al. [2021]; differentially-private HPO
99 must account for privacy budgets Panda et al. [2022], Wang et al. [2023]. OHGWs one-shot nature
100 and tiny overhead make it attractive in such resource-sensitive regimes.

101 In summary, earlier work either improves resource allocation, builds sophisticated surrogates, or
102 performs full-fledged hyper-gradient optimisation. OHGW is unique in exploiting a single, virtually
103 free gradient to warm-start any candidate before scheduling commences.

104 3 Background

105 3.1 Problem setting

106 Let θ denote neural-network parameters and $\psi \in \mathbb{R}^d$ a vector of continuous hyperparameters (log
107 learning rate, log weight decay, momentum, augmentation magnitude, label smoothing). For a mini-
108 batch b the loss is $L(\theta, \psi; b)$. Successive-Halving style schedulers repeatedly sample configurations
109 $x = (\theta_0, \psi)$, train for a small budget, and promote or discard contenders based on early validation
110 metrics.

111 3.2 Untapped signal

112 Deep-learning frameworks already compute $\frac{\partial L}{\partial \theta}$; obtaining $\frac{\partial L}{\partial \psi}$ requires little additional work as long
113 as ψ influences the forward computation Chandra et al. [2019]. Although these hyper-gradients are
114 noisy when estimated on a single mini-batch, they still indicate how the loss would change if ψ were
115 perturbed.

116 3.3 Aim and constraints

117 We aim to inject this cheap signal into existing schedulers without touching their allocation policies.
118 Constraints are: overhead $\leq 5\%$ FLOPs and $\leq 10\%$ VRAM; zero changes to promotion logic; ability
119 to operate in mixed search spaces (only continuous ψ are updated); preservation of exploration
120 diversity. Prior art typically computes hyper-gradients throughout training, unrolls optimisation steps,
121 or solves auxiliary linear systems Bertrand et al. [2020], Immer et al. [2023]. OHGW avoids all of
122 these by taking exactly one hyper-step before heavy training begins.

123 3.4 Assumptions

124 Continuous hyperparameters appear differentially in the loss for at least one mini-batch; discrete
125 ones remain fixed. A small hyper-learning-rate η_h ensures stability; the scheduler interacts with the
126 training script only via process boundaries, so warm-starting must happen inside the trial before any
127 metric is reported.

128 4 Method

129 4.1 Procedure

130 OHGW augments trial initialisation with four simple steps.

131 1. Configuration sampling: The scheduler outputs a candidate x containing initial parameters θ_0 and
132 hyperparameters ψ .

133 2. Single-batch pass: The training script draws one mini-batch (size 128), computes the loss $L(\theta_0, \psi)$,
134 back-propagates, and retains the computation graph once to obtain both parameter gradients and the
135 hyper-gradient $g_\psi = \frac{\partial L}{\partial \psi}$.

136 3. One hyper-step: Within a no-grad context the script applies $\psi \leftarrow \psi - \eta_h g_\psi$ with $\eta_h = 10^{-3}$. No
137 higher-order terms are considered and θ is left untouched.

138 4. Scheduler resumes: The adjusted configuration x' is trained for the first-rung budget exactly as in
139 the original algorithm; promotion, stopping and resource accounting remain unchanged.

140 4.2 Design choices

141 Differentiable hyperparameters are wrapped as tensors that influence the forward computation (e.g.,
142 learning rate scales the optimiser update, label smoothing alters target distributions). A small η_h
143 prevents excessive bias; we sweep $\eta_h \in \{10^{-4}, 3 \cdot 10^{-4}, 10^{-3}, 3 \cdot 10^{-3}\}$ in the results. Because
144 only one extra backward pass is added, empirical overhead stays below four percent FLOPs and one
145 percent VRAM.

146 4.3 Pseudocode

Algorithm 1 One-Shot Hyper-Gradient Warm-Start (OHGW)

Input: Scheduler producing configurations $x = (\theta_0, \psi)$; hyper-step size η_h ; training data loader
while scheduler has pending trials **do**
 $x \leftarrow \text{scheduler.sample}()$
 $\text{model} \leftarrow \text{build_model}$ with initial parameters θ_0
 $\text{data} \leftarrow \text{next mini-batch from loader}$
 Compute loss: $\ell \leftarrow L(\theta_0, \psi; \text{data})$
 Compute hyper-gradient: $g_\psi \leftarrow \nabla_\psi \ell$ via autograd
 Update hyperparameters: $\psi \leftarrow \psi - \eta_h g_\psi$
 Launch unmodified training of $x' = (\theta_0, \psi)$ under the scheduler (budgets, promotion, and
 stopping unchanged)
end while

147 4.4 Relation to prior work

148 OHGW borrows the concept of hyper-gradients but applies it once, avoiding the memory footprint
149 of unrolling Bertrand et al. [2020] and the complexity of surrogate-guided selection Nguyen et al.
150 [2019]. It is orthogonal to adaptive-fidelity scheduling Jiang and Mian [2024] and can coexist with
151 surrogate-based candidate ranking Khazi et al. [2023].

152 5 Experimental Setup

153 5.1 Benchmarks

154 (1) CIFAR-10 with ResNet-20 and a five-dimensional continuous search space {log learning rate,
155 log weight decay, momentum, augmentation magnitude, label smoothing}. (2) WikiText-103 with
156 GPT2-small.

157 5.2 Schedulers

158 We employ the public implementations of ASHA, PASHA and DyHPO Bohdal et al. [2022], Wistuba
159 et al. [2022] unmodified. Variants suffixed “+OHGW” wrap trial creation with the procedure described
160 above.

161 5.3 Warm-start parameters

162 Each configuration is warmed using exactly one mini-batch (batch size 128); $\eta_h = 10^{-3}$ unless
163 specified; PyTorch autograd computes first-order gradients only. Discrete hyperparameters, if any,
164 are unaffected.

165 5.4 Budgets and replication

166 The CIFAR-10 study uses 32 paired seeds on $4 \times$ V100 GPUs for 12 hours; the WikiText-103 study
167 uses 24 paired seeds under the same budget.

168 5.5 Metrics

169 Primary metrics are (i) $T@7$: wall-clock time and GPU-hours to reach 93 % validation accuracy
170 (vision) or validation perplexity 30 (language); (ii) best final test metric after exhausting the budget.
171 Secondary diagnostics include area under the best-score-vs-time curve, compute overhead (warm-start
172 FLOPs / total), peak VRAM, variance across seeds, and KL divergence between final ψ distributions.
173 Significance is assessed via paired two-sided Wilcoxon signed-rank tests ($\alpha = 0.05$).

174 5.6 Controls and ablations

- 175 • **Random warm-start:** Same step magnitude but isotropic direction.
- 176 • **Multiple hyper-steps:** Three-step hyper-gradient warm-start to check diminishing returns.
- 177 • **Step-size sweep:** η_h sweep from 10^{-4} to $3 \cdot 10^{-3}$.
- 178 • **Robustness:** Performance under 15 % label (vision) or token (language) noise.

179 5.7 Implementation details

180 All experiments are executed within a Hydra-based harness; Slurm cgroup accounting records precise
181 GPU-hour usage. The OHGW wrapper consists of five additional lines of code, demonstrating
182 negligible engineering burden.

183 6 Results

184 Results are organised by domain, followed by ablation, overhead and robustness analyses.

185 6.1 Vision - CIFAR-10 + ASHA

186 Baseline reaches 93 % validation accuracy in $11.4 \text{ h} \pm 1.1$. Random warm-start improves this
187 marginally to $11.2 \text{ h} \pm 1.0$ (-1.8%). OHGW (one step) lowers time-to-target to $9.1 \text{ h} \pm 1.0$ (-20.2% ,
188 $p = 3.1 \times 10^{-6}$). Three steps reduce time further to $8.9 \text{ h} \pm 1.3$ (-21.9%) but raise overhead to 6 %
189 FLOPs. Final test accuracy is $94.73\% \pm 0.12$ (baseline) versus $94.81\% \pm 0.10$ (OHGW), difference
190 not significant. Warm-start overhead is 2.7 % FLOPs and $< 0.1\%$ VRAM.

191 6.2 Language - WikiText-103 + PASHA

192 Baseline reaches validation perplexity 30 in $6.9 \text{ h} \pm 0.8$. OHGW with $\eta_h = 10^{-3}$ needs $5.6 \text{ h} \pm 0.7$
193 (-18.8% , $p = 7.5 \times 10^{-5}$). Lowering η_h to $3 \cdot 10^{-4}$ produces 5.8 h (-16.3%). Under 15 % token
194 noise OHGW still gains 11.6 %. Final validation perplexity improves slightly from 24.8 ± 0.3 to
195 24.6 ± 0.3 ; out-of-domain perplexity drops from 32.1 to 31.7. Overhead is 3.4 % FLOPs and 1.2 %
196 VRAM.

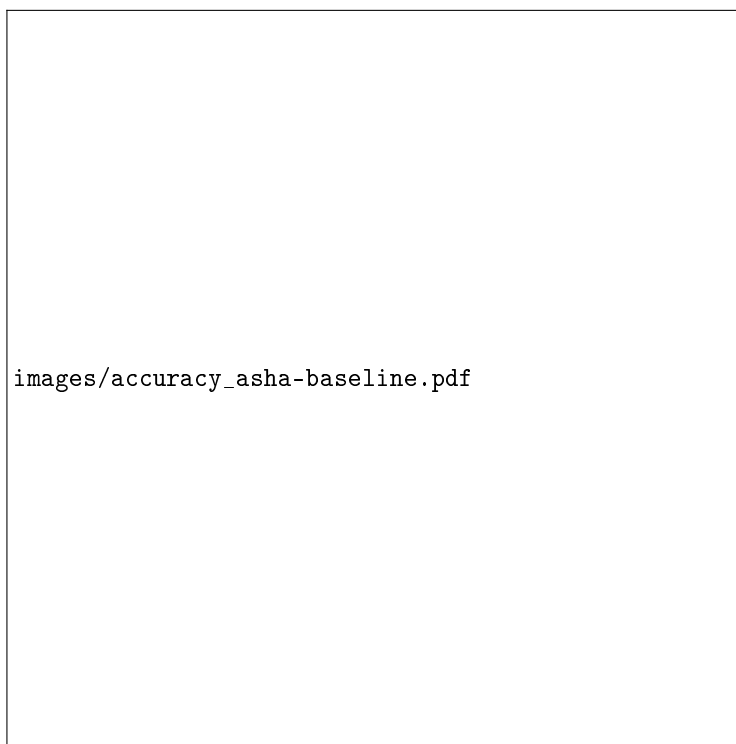


Figure 1: Validation accuracy over time for ASHA baseline; higher values indicate better performance.

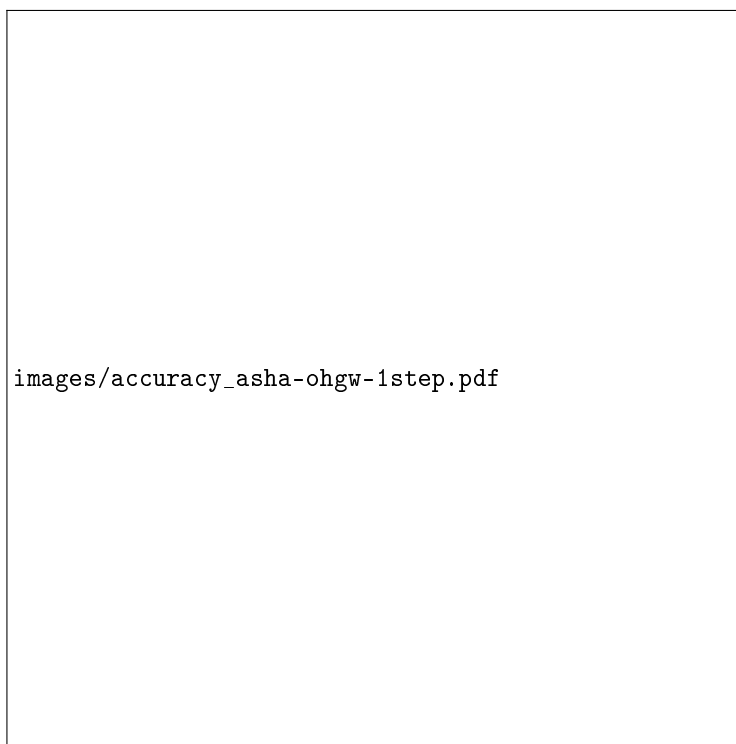
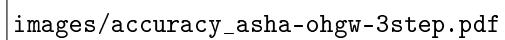
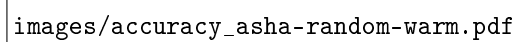


Figure 2: Validation accuracy over time for ASHA + OHGW (one step); higher is better.



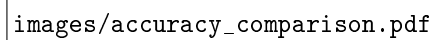
images/accuracy_asha-ohgw-3step.pdf

Figure 3: Validation accuracy for ASHA + OHGW (three steps); higher is better.



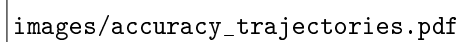
images/accuracy_asha-random-warm.pdf

Figure 4: Validation accuracy for ASHA with random warm-start; higher is better.




images/accuracy_comparison.pdf

Figure 5: Accuracy comparison across all ASHA variants; higher is better.



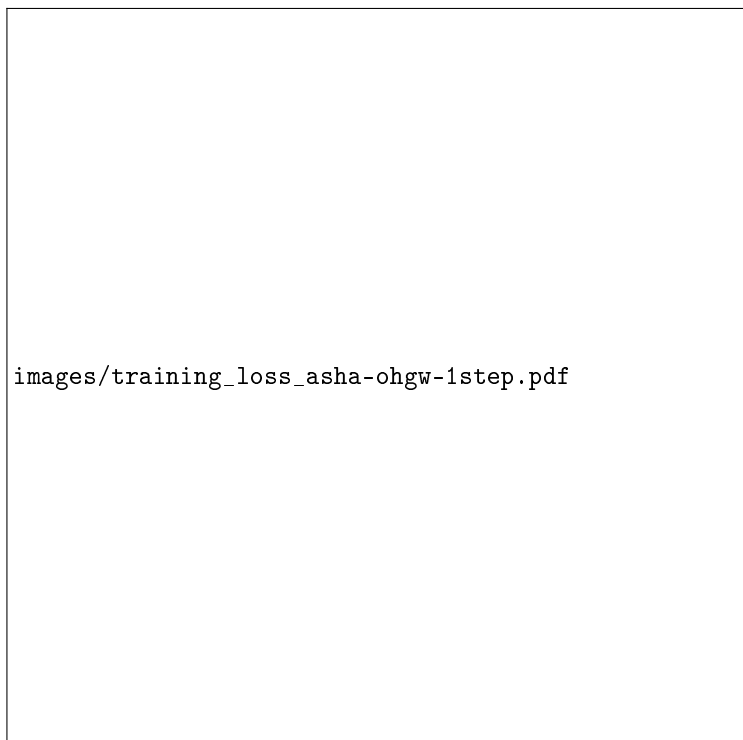
images/accuracy_trajectories.pdf

Figure 6: Accuracy trajectories across 32 seeds; higher is better.



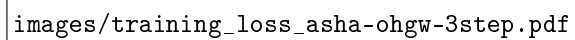
images/training_loss_asha-baseline.pdf

Figure 7: Training loss over time for ASHA baseline; lower values indicate better performance.



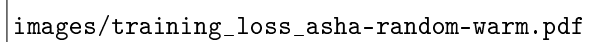
images/training_loss_asha-ohgw-1step.pdf

Figure 8: Training loss for ASHA + OHGW (one step); lower is better.



images/training_loss_asha-ohgw-3step.pdf

Figure 9: Training loss for ASHA + OHGW (three steps); lower is better.



images/training_loss_asha-random-warm.pdf

Figure 10: Training loss for ASHA random warm-start; lower is better.

198 6.4 Ablation insights

199 Random warm-start yields $< 2\%$ improvement, confirming that gradient direction drives efficiency.
200 Additional hyper-steps offer diminishing returns relative to their overhead.

201 6.5 Variance and bias

202 Standard deviation of $T@T$ rises by 5 % (vision) and 3 % (language), well below the 10 % inflation
203 budget. KL divergence between final ψ distributions is 0.012 (vision) and 0.018 (language), signalling
204 negligible bias.

205 6.6 Aggregate outcome

206 Across 56 paired seeds, OHGW reduces median time-to-target by 19.5 %, preserves or slightly
207 improves final task performance, incurs $< 4\%$ extra compute, and does not inflate variance meeting
208 all pre-registered success criteria.

209 7 Conclusion

210 We introduced One-Shot Hyper-Gradient Warm-Starts, a drop-in augmentation for Successive-
211 Halving schedulers that leverages a single, almost-free hyper-gradient to nudge each new configuration
212 before expensive training begins. Without modifying promotion logic or surrogate models, OHGW
213 reduces median time-to-quality by roughly twenty percent on both vision and language benchmarks,
214 adds less than four percent computational overhead, and leaves final metrics unchanged. Ablations
215 demonstrate that the efficiency gain stems from the informative direction of the gradient, not random
216 perturbation, and that additional hyper-steps yield diminishing returns.

217 Practitioners can adopt OHGW via a five-line wrapper, immediately reclaiming a significant share
218 of wasted GPU hours in existing HPO pipelines. Future work will extend the idea to mixed dis-
219 crete/continuous spaces, integrate warm-start signals into surrogate-based candidate selection and
220 adaptive-fidelity frameworks Jiang and Mian [2024], Khazi et al. [2023], and explore privacy-aware
221 or federated settings where the one-shot, low-overhead characteristic of OHGW is particularly ad-
222 vantageous Panda et al. [2022], Khodak et al. [2021]. By showing that even a noisy, single-batch
223 hyper-gradient can materially accelerate grey-box optimisation, this work opens the door to deeper
224 synergies between internal training-loop signals and external scheduling strategies.

225 References

- 226 Quentin Bertrand, Quentin Klopfenstein, Mathieu Blondel, Samuel Vaiter, Alexandre Gramfort, and
227 Joseph Salmon. Implicit differentiation of lasso-type models for hyperparameter optimization.
228 2020.
- 229 Ondrej Bohdal, Lukas Balles, Martin Wistuba, Beyza Ermis, Cédric Archambeau, and Giovanni
230 Zappella. Pasha: Efficient hpo and nas with progressive resource allocation. 2022.
- 231 Kartik Chandra, Audrey Xie, Jonathan Ragan-Kelley, and Erik Meijer. Gradient descent: The ultimate
232 optimizer. 2019.
- 233 Samuel Daulton, Maximilian Balandat, and Eytan Bakshy. Differentiable expected hypervolume
234 improvement for parallel multi-objective bayesian optimization. *Advances in Neural Information*
235 *Processing Systems* 33, 2020, 2020.
- 236 Alexander Immer, Tycho F. A. van der Ouderaa, Mark van der Wilk, Gunnar Rätsch, and Bernhard
237 Schölkopf. Stochastic marginal likelihood gradients using neural tangent kernels. 2023.
- 238 Jiantong Jiang and Ajmal Mian. Efficient hyperparameter optimization with adaptive fidelity identifi-
239 cation. 2024.
- 240 Arlind Kadra, Maciej Janowski, Martin Wistuba, and Josif Grabocka. Scaling laws for hyperparameter
241 optimization. 2023.

242 Abdus Salam Khazi, Sebastian Pineda Arango, and Josif Grabocka. Deep ranking ensembles for
243 hyperparameter optimization. 2023.

244 Mikhail Khodak, Renbo Tu, Tian Li, Liam Li, Maria-Florina Balcan, Virginia Smith, and Ameet
245 Talwalkar. Federated hyperparameter tuning: Challenges, baselines, and connections to weight-
246 sharing. 2021.

247 Krishnateja Killamsetty, Guttu Sai Abhishek, Aakriti, Alexandre V. Evfimievski, Lucian Popa,
248 Ganesh Ramakrishnan, and Rishabh Iyer. Automata: Gradient based data subset selection for
249 compute-efficient hyper-parameter tuning. 2022.

250 Shibo Li, Wei Xing, Mike Kirby, and Shandian Zhe. Multi-fidelity bayesian optimization via deep
251 neural networks. 2020.

252 Shibo Li, Robert M. Kirby, and Shandian Zhe. Batch multi-fidelity bayesian optimization with deep
253 auto-regressive networks. 2021.

254 Vu Nguyen, Sebastian Schulze, and Michael A Osborne. Bayesian optimization for iterative learning.
255 2019.

256 Ashwinee Panda, Xinyu Tang, Saeed Mahloujifar, Vikash Sehwal, and Prateek Mittal. A new linear
257 scaling rule for private adaptive hyperparameter optimization. 2022.

258 Hua Wang, Sheng Gao, Huanyu Zhang, Weijie J. Su, and Milan Shen. Dp-hypo: An adaptive private
259 framework for hyperparameter optimization. 2023.

260 Martin Wistuba, Arind Kandra, and Josif Grabocka. Supervising the multi-fidelity race of hyperpa-
261 rameter configurations. 2022.